

Evidence for an excitonic insulator phase in 1T-TiSe₂

H. Cercellier,* C. Monney, F. Clerc, C. Battaglia, L. Despont, M. G. Garnier, H. Beck, and P. Aebi
Institut de Physique, Université de Neuchâtel, CH-2000 Neuchâtel, Switzerland

L. Patthey
Swiss Light Source, Paul Scherrer Institute, CH-5232 Villigen, Switzerland

H. Berger
Institut de Physique de la Matière Complexe, EPFL, CH-1015 Lausanne, Switzerland
 (Dated: February 13, 2013)

We present a new high-resolution angle-resolved photoemission study of 1T-TiSe₂ in both, its room-temperature, normal phase and its low-temperature, charge-density wave phase. At low temperature the photoemission spectra are strongly modified, with large band renormalisations at high-symmetry points of the Brillouin zone and a very large transfer of spectral weight to backfolded bands. A theoretical calculation of the spectral function for an excitonic insulator phase reproduces the experimental features with very good agreement. This gives strong evidence in favour of the excitonic insulator scenario as a driving force for the charge-density wave transition in 1T-TiSe₂.

PACS numbers:

Transition-metal dichalcogenides (TMDC's) are layered compounds exhibiting a variety of interesting physical properties, mainly due to their reduced dimensionality [1]. One of the most frequent characteristics is a ground state exhibiting a charge-density wave (CDW), with its origin arising from a particular topology of the Fermi surface and/or a strong electron-phonon coupling [2]. Among the TMDC's 1T-TiSe₂ shows a commensurate 2×2×2 structural distortion below 202 K, accompanied by the softening of a zone boundary phonon and with changes in the transport properties [3, 4]. In spite of many experimental and theoretical studies, the driving force for the transition remains controversial. Several angle-resolved photoelectron spectroscopy (ARPES) studies suggested either the onset of an excitonic insulator phase [5, 6] or a band Jahn-Teller effect [7]. Furthermore, TiSe₂ has recently attracted strong interest due to the observation of superconductivity when intercalated with Cu [8]. In systems showing exotic properties, such as Kondo systems for example [9], the calculation of the spectral function has often been a necessary and decisive step for the interpretation of the ARPES data and the determination of the ground state of the systems. In the case of 1T-TiSe₂, such a calculation for an excitonic insulator phase lacked so far.

In this letter we present a high-resolution ARPES study of 1T-TiSe₂, together with theoretical calculations of the excitonic insulator phase spectral function for this compound. We find that the experimental ARPES spectra show strong band renormalisations with a very large transfer of spectral weight into backfolded bands in the low-temperature phase. The spectral function calculated for the excitonic insulator phase is in strikingly good

agreement with the experiments, giving strong evidence for the excitonic origin of the transition.

The excitonic insulator model was first introduced in the sixties, for a semi-conductor or a semi-metal with a very small indirect gap E_G [10, 11, 12, 13]. Thermal excitations lead to the formation of holes in the valence band and electrons in the conduction band. For low free carrier densities, the weak screening of the electron-hole Coulomb interaction leads to the formation of stable electron-hole bound states, called excitons. If the exciton binding energy E_B is larger than the gap energy E_G , the system becomes unstable upon formation of excitons. This instability can drive a transition to a coherent ground state of condensed excitons, with a periodicity given by the spanning vector \mathbf{w} that connects the valence band maximum to the conduction band minimum. In the particular case of TiSe₂, there are three vectors (\mathbf{w}_i , $i = 1, 2, 3$) connecting the Se 4p-derived valence band maximum at the Γ point to the three symmetry-equivalent Ti 3d-derived conduction band minima at the L points of the Brillouin zone (BZ) (see inset of fig. 1b)).

Our calculations are based on the BCS-like model of Jérôme, Rice and Kohn [12], adapted for multiple \mathbf{w}_i . The band dispersions for the normal phase have been chosen of the form

$$\begin{aligned}\epsilon_v(\mathbf{k}) &= \epsilon_v^0 + \hbar^2 \frac{k_x^2 + k_y^2}{2m_v} + t_v \cos\left(\frac{2\pi k_z}{c}\right) \\ \epsilon_c^i(\mathbf{k}, \mathbf{w}_i) &= \epsilon_c^0 + \hbar^2 \left(\frac{(k_x - w_{ix})^2}{2m_c^x} + \frac{(k_y - w_{iy})^2}{2m_c^y} \right) \\ &\quad + t_c \cos\left(\frac{2\pi(k_z - w_{iz})}{c}\right)\end{aligned}\quad (1)$$

for the valence (ϵ_v) and the three conduction (ϵ_c^i) bands respectively, with c the lattice parameter perpendicular to the surface in the normal (1×1×1) phase, t_v and t_c the amplitudes of the respective dispersions perpendicular to the surface and m_v , m_c the effective masses.

*Electronic address: herve.cercellier@unine.ch

The parameters for equations 1 were derived from photon energy dependent ARPES measurements carried out at the Swiss Light Source on the SIS beamline, using a Scienta SES-2002 spectrometer with an overall energy resolution better than 10 meV, and an angular resolution better than 0.5° . The fit to the data gives for the Se 4p valence band maximum -20 ± 10 meV, and for the Ti 3d conduction band a minimum -40 ± 5 meV [14]. From our measurements we then find a semimetallic band structure with a negative gap (*i.e.* an overlap) $E_G = -20 \pm 15$ meV for the normal phase of TiSe_2 , in agreement with the literature [15]. The dispersions deduced from the ARPES data are shown in fig. 1a) (dashed lines).

Within this model the one-electron Green's functions of the valence and the conduction bands were calculated for the excitonic insulator phase. For the valence band, one obtains

$$G_v(\mathbf{k}, z) = \left(z - \epsilon_v(\mathbf{k}) - \sum_{\mathbf{w}_i} \frac{|\Delta|^2(\mathbf{k}, \mathbf{w}_i)}{z - \epsilon_c(\mathbf{k} + \mathbf{w}_i)} \right)^{-1}. \quad (2)$$

This is a generalized form of the equations of Ref. [12] for an arbitrary number of \mathbf{w}_i . The order parameter Δ is related to the number of excitons in the condensed state at a given temperature. For the conduction band, there is a system of equations describing the Green's functions G_c^i corresponding to each spanning vector vector \mathbf{w}_i :

$$\begin{aligned} [z - \epsilon_c^i(\mathbf{k} + \mathbf{w}_i)] G_c^i(\mathbf{k} + \mathbf{w}_i, z) &= 1 + \Delta^*(\mathbf{k}, \mathbf{w}_i) \\ &\times \sum_j \frac{\Delta(\mathbf{k}, \mathbf{w}_j) G_c^j(\mathbf{k} + \mathbf{w}_j, z)}{z - \epsilon_v(\mathbf{k})} \end{aligned} \quad (3)$$

This model and the derivation of the Green's functions will be further described elsewhere [16].

The spectral function calculated along several high-symmetry directions of the BZ is shown in fig. 1a) for an order parameter $\Delta = 0.05$ eV. Its value has been chosen for best agreement with experiment. The color scale shows the spectral weight carried by each band. For presentation purposes the δ -like peaks of the spectral function have been broadened by adding a constant 30 meV imaginary part to the self-energy. In the normal phase (dashed lines), as previously described we consider a semimetal with a 20 meV overlap, with bands carrying unity spectral weight. In the excitonic phase, the band structure is strongly modified. The first observation is the appearance of new bands (labeled C1, V2 and C3), backfolded with the spanning vector $\mathbf{w} = \Gamma L$. The C1, V2 and C3 branches are the backfolded replicas of branches C2, V3 and C4 respectively. In this new phase the Γ and L points are now equivalent, which means that the excitonic state has a $2 \times 2 \times 2$ periodicity of purely electronic origin, as expected from theoretical considerations [10, 12]. Another effect of exciton condensation is the opening of a gap in the excitation spectrum. This results in a flattening of the valence band near Γ in the ΓM direction (V1 branch) and in the $A\Gamma$ direction (V3 branch), and also an upward bend of the conduction band near L and M (C2 and C4

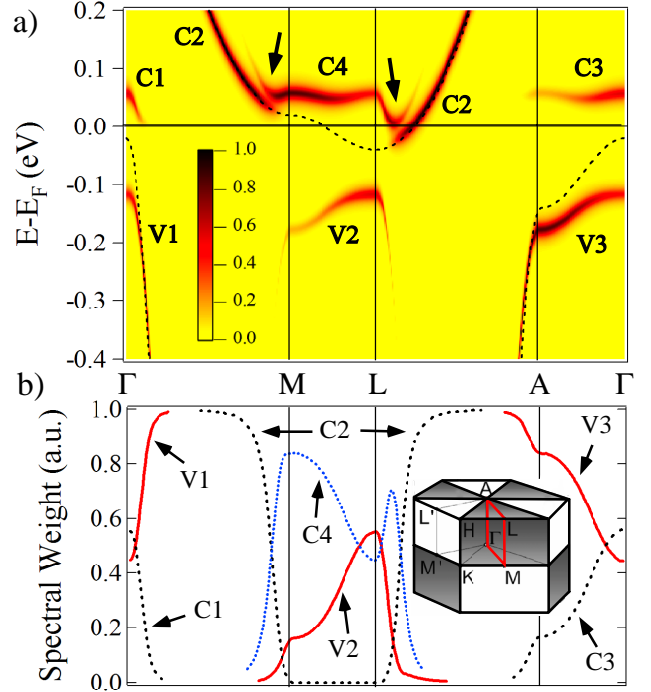


FIG. 1: a) Spectral function of the excitonic insulator in a 1T structure calculated for a 20 meV overlap and an order parameter $\Delta = 0.05$ eV. The V1-V3 (resp. C1-C4) branches refer to the valence (resp. conduction) band. Dashed lines correspond to the normal phase ($\Delta = 0$). The path in reciprocal space is shown in red in the inset. b) Spectral weight of the different bands. Inset : bulk Brillouin zone of 1T- TiSe_2 .

branches). It is interesting to notice that in the vicinity of these two points, the conduction band is split (arrows). This results from the backfolding of the L points onto each other, according to the new periodicity of the excitonic state [17]. The spectral weight carried by the bands is shown in fig. 1b). The largest variations occur near the Γ , L and M points, where the band extrema in the normal phase are close enough for excitons to be created. Away from these points, the spectral weight decreases in the backfolded bands (C1, V2, C3) and increases in the others. The intensity of the V1 branch, for example, decreases by a factor of 2 when approaching Γ , whereas the backfolded C1 branch shows the opposite behaviour. Such a large transfer of spectral weight into the backfolded bands is a very uncommon and striking feature. Indeed, in most compounds with competing potentials (CDW systems, vicinal surfaces,...), the backfolded bands carry an extremely small spectral weight [18, 19, 20]. In these systems the backfolding results mainly from the influence of the modified lattice on the electron gas, and the weight transfer is related to the strength of the new crystal potential component. Here, the case of the excitonic insulator is completely different, as the backfolding is an intrinsic property of the excitonic state. The large

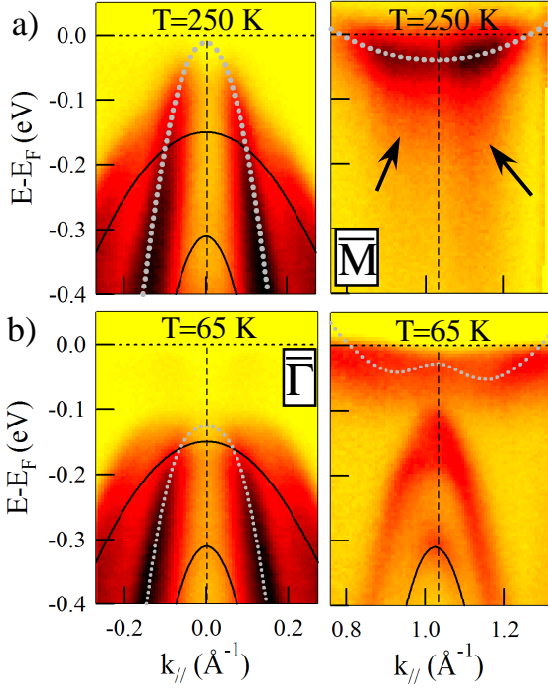


FIG. 2: : ARPES spectra of 1T-TiSe₂ for a) the normal and b) the low temperature phase. Thick dotted lines are parabolic fits to the bands in the normal phase and thin dotted lines are guides to the eye for the CDW phase. Fine lines follow the dispersion of the 4p sidebands (see text).

transfer of spectral weight is then a purely electronic effect, and turns out to be a characteristic feature of the excitonic insulator phase.

Fig. 2 shows ARPES spectra recorded at a photon energy $h\nu=31$ eV as a function of temperature. At this photon energy, the normal emission spectra correspond to states located close to the Γ point. For the sake of simplicity the description is in terms of the surface BZ high-symmetry points $\bar{\Gamma}$ and \bar{M} . The 250 K spectra exhibit the three Se 4p-derived bands at $\bar{\Gamma}$ and the Ti 3d-derived band at \bar{M} widely described in the literature [5, 6, 7]. The thick dotted lines (white) are fits by equation 1, giving for the topmost 4p band a maximum energy of -20 ± 10 meV, and for the Ti 3d a minimum energy of -40 ± 5 meV. The small overlap $E_G = -20 \pm 15$ meV in the normal phase is consistent with the excitonic insulator scenario, as the exciton binding energy is expected to be close to that value. [5, 6]. The position of both band maxima in the occupied states is most probably due to a slight Ti overdoping of our samples [3]. In our case, a transition temperature of 180 ± 10 K was found from different ARPES and scanning tunneling microscopy measurements, indicating a Ti doping of less than 1 %. On the 250 K spectrum at $\bar{\Gamma}$, the intensity is low near normal emission. This reduced intensity and the residual intensity at \bar{M} around 150 meV binding energy (arrows) may arise from exciton fluctuations (see reduction of spectral

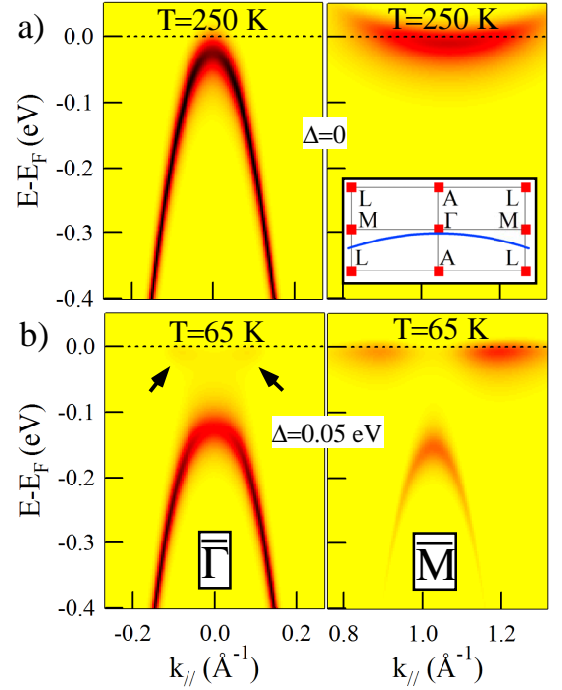


FIG. 3: : Theoretical spectral function of 1T-TiSe₂, calculated along the path given by the free electron final state approximation shown in the inset. a) normal state and b) low temperature phase (see text).

weight near Γ in the V1 branch in fig. 1b). Matrix elements do not appear to play a role as the intensity variation only depends very slightly on photon energy and polarization. In the 65 K data (fig. 2b)), the topmost 4p band flattens near $\bar{\Gamma}$ and shifts to higher binding energy by about 100 meV (thin white, dotted line). This shift is accompanied by a larger decrease of the spectral weight near the top of the band. The two other bands (fine black lines) are only slightly shifted and do not appear to participate in the transition. In the \bar{M} spectrum strong backfolded valence bands can be seen, and the conduction band bends upwards, leading to a maximum intensity located about 0.25 \AA^{-1} from \bar{M} (thin white dotted line). This observation is in agreement with Kidd *et al.* [6], although in their case the conduction band was unoccupied in the normal phase.

The calculated spectral functions corresponding to the data of fig. 2 are shown in fig. 3, using the free-electron final state approximation with a 10 eV inner potential and a 4.6 eV work function (see inset). The effect of temperature was taken into account via the order parameter and the Fermi function. Only the topmost valence band was considered, as the other two are practically not influenced by the transition (see above, fig. 2). The behavior of this band is extremely well reproduced by the calculation. In the 65 K calculation the valence band is flattened near $\bar{\Gamma}$, and the spectral weight at this point is reduced to 44 %, close to the experimental value of 35 %. The agreement

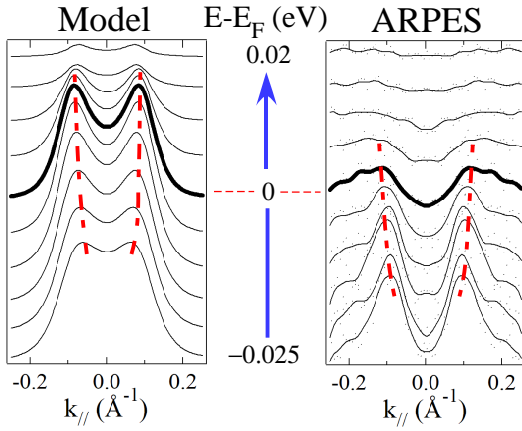


FIG. 4: : Near- E_F constant energy cuts in the vicinity of the Γ point. The theoretical data correspond to fig. 3b and the ARPES data are taken from the low-temperature data of fig. 2b.

is very satisfying, considering that the calculation takes into account only the lowest excitonic state. The experimental features appear broader than in the calculation, but at finite temperatures one may expect the existence of excitons with non-zero momentum, leading to a spread of spectral weight away from the high-symmetry points.

In the near- \bar{M} spectral function, the backfolded valence band is strongly present in the 65 K calculation, with comparable spectral weight as at $\bar{\Gamma}$ and as the conduction band at \bar{M} . The conduction band maximum intensity is located away from \bar{M} as in the experiment. The small perpendicular dispersion of the free-electron final state causes an asymmetry of the intensity of the conduction band on each side of \bar{M} , which is also visible in fig. 2. In our calculation, as opposed to the ARPES spectra, the conduction band is unoccupied and only the occupied tail of the peaks is visible. This difference may be simply due to the final state approximation used in the calculation, a slight shift of the chemical potential due to the transition, or to atomic displacements that

would shift the conduction band [6, 7, 21]. Such atomic displacements, in terms of a band Jahn-Teller effect, were suggested as a driving force for the transition. However, the key point is that, although the lattice distortion may shift the conduction band, the very small atomic displacements (≈ 0.02 Å [3]) in 1T-TiSe₂ are expected to lead to a negligible spectral weight in the backfolded bands [20]. As an example, 1T-TaS₂, another CDW compound known for very large atomic displacements [22] (of order > 0.1 Å) introduces hardly detectable backfolding of spectral weight in ARPES. Clearly, an electronic origin is necessary for obtaining such strong backfolding in the presence of such small atomic displacements. Therefore, our results allow to rule out a Jahn-Teller effect as the driving force for the transition of TiSe₂.

Furthermore, the ARPES spectra also show evidence for the backfolded conduction band at the $\bar{\Gamma}$ point. Fig. 4 shows constant energy cuts around the Fermi energy, taken from the data of fig. 2b and 3b (arrows). In the ARPES data two slightly dispersive peaks, reproduced in the calculation, clearly cross the Fermi level. These features turn out to be the populated tail of the backfolded conduction band, whose centroid is located just above the Fermi level. To our knowledge no evidence for the backfolding of the conduction band had been put forward so far.

In summary, by comparing ARPES spectra of 1T-TiSe₂ to theoretical predictions for an excitonic insulator, we have shown that the superperiodicity of the excitonic state with respect to the lattice results in a very large transfer of spectral weight into backfolded bands. This effect, clearly evidenced by photoemission, turns out to be a characteristic feature of the excitonic insulator phase, thus giving strong evidence for the existence of this phase in 1T-TiSe₂ and its prominent role in the CDW transition.

Skillfull technical assistance was provided by the workshop and electric engineering team. This work was supported by the Fonds National Suisse pour la Recherche Scientifique through Div. II and MaNEP.

-
- [1] J. A. Wilson *et al.*, Adv. Phys. **24**, 117 (1975).
 - [2] F. Clerc *et al.*, Phys. Rev. B **74**, 155114 (2006).
 - [3] F. J. Di Salvo *et al.*, Phys. Rev. B **14**, 4321 (1976).
 - [4] M. Holt *et al.*, Phys. Rev. Lett. **86**, 3799 (2001).
 - [5] T. Pillo *et al.*, Phys. Rev. B **61**, 16213 (2000).
 - [6] T. E. Kidd *et al.*, Phys. Rev. Lett. **88**, 226402 (2002).
 - [7] K. Rossnagel *et al.*, Phys. Rev. B **65**, 235101 (2002).
 - [8] E. Morosan *et al.*, Nature Physics **2**, 544 (2006).
 - [9] D. Malterre *et al.*, Adv. Phys. **45**, 299 (1996).
 - [10] W. Kohn, Phys. Rev. Lett. **19**, 439 (1967).
 - [11] B. I. Halperin and T. M. Rice, Rev. Mod. Phys. **40**, 755 (1968).
 - [12] D. Jérôme *et al.*, Phys. Rev. **158**, 462 (1967).
 - [13] F. X. Bronold and H. Fehske, Phys. Rev. B **74**, 165107 (2006).
 - [14] The fit parameters are : $\epsilon_v^0 = -0.08 \pm 0.005$ eV, $m_v = -0.23 \pm 0.02$ m_e , where m_e is the free electron mass, $t_v = 0.06 \pm 0.005$ eV ; $\epsilon_c^0 = -0.01 \pm 0.0025$ eV, $m_c^x = 5.5 \pm 0.2$ m_e , $m_c^y = 2.2 \pm 0.1$ m_e , $t_c = 0.03 \pm 0.0025$ eV
 - [15] O. Anderson *et al.*, Phys. Rev. Lett. **55**, 2188 (1985).
 - [16] C. Monney *et al.*, to be published
 - [17] J. A. Wilson *et al.*, Phys. Rev. B **18**, 2866 (1978).
 - [18] C. Didiot *et al.*, Phys. Rev. B **74**, 081404(R) (2006).
 - [19] C. Battaglia *et al.*, Phys. Rev. B **72**, 195114 (2005).
 - [20] J. Voit *et al.*, Science **290**, 501 (2000).
 - [21] M. H. Whangbo and E. Canadell, J. Am. Chem. Soc. **114**, 9587 (1992).
 - [22] A. Spijkerman *et al.*, Phys. Rev. B **56**, 13757 (1997).